The Astrophysical Journal, 653:719–724, 2006 December 10

HARD X-RAY PRODUCTION IN A FAILED FILAMENT ERUPTION

David Alexander, Rui Liu, and Holly R. Gilbert
Department Physics and Astronomy, Rice University, 6100 Main Street, Houston TX 77005; dalex@rice.edu
Received 2006 April 17; accepted 2006 July 27

ABSTRACT

We revisit the "failed" filament eruption of 2002 May 27, first studied in detail by Ji et al. We investigate the temporal and spatial relationship between the filament dynamics and the production of hard X-ray emission using spatially resolved high-cadence data from *TRACE* and *RHESSI*. We confirm the presence of a hard X-ray source in the corona above the filament prior to the main activation phase and identify a second coronal hard X-ray source, not considered by earlier studies, that occurs under the apex of the filament during the erupting phase when the filament is clearly strongly kinked. We argue that this second source of coronal hard X-ray emission implies ongoing magnetic reconnection in a current sheet formed via a kink instability resulting from the interaction of the two adjacent legs underneath the writhing filament, in agreement with simulation results. The presence of this second energy release site has important implications for models of solar eruptions.

Subject headings: Sun: coronal mass ejections (CMEs) — Sun: magnetic fields — Sun: prominences — Sun: X-rays, gamma rays

Online material: color figure, mpeg animations

1. INTRODUCTION

The importance of filament activity as a driver of space weather phenomena is a critical topic in solar physics. Solar filament eruptions are frequently associated with coronal mass ejections (CMEs) and solar flares, with all three phenomena generally occurring together in the largest events. This direct association suggests a commonality of the physical processes driving these disparate phenomena, a commonality that has been exploited to good effect by models of CME and flare initiation (see review by Lin et al. 2003). Recently, however, there has been much study of the nature of filament activation and its role in driving solar transient phenomena (e.g., Martin 1998; Gilbert et al. 2000).

Filament activation encompasses a wide array of phenomena, including partial and so-called failed eruptions. The partial eruptions of solar filaments are frequently observed to occur (Pevtsov 2002; Gilbert et al. 2001) and are generally accompanied by flaring activity in the solar corona. Failed eruptions (e.g., Ji et al. 2003; hereafter J03) are defined by the dynamical evolution of the filament, which displays an initially eruptive-like acceleration persisting for a relatively short duration prior to a period in which the filament decelerates, reaching a maximum height as the mass in the filament threads drains back toward the Sun. Such events can produce solar flares, but generally are not associated with CMEs nor show much evidence for the opening of the magnetic field.

There is clearly a range of eruptive-like dynamic activity in filaments, from full eruption through partial eruption to failed eruption. The importance of the dynamic nature of filaments to the potential for eruption and CME initiation is still being explored, but the interaction between the filament magnetic field and the dynamical motions is such that any external disturbance, such as emerging or canceling flux in the filament vicinity, could have dramatic consequences for the filament itself. Sterling et al. (2001) used observations of Hα filament activation in the buildup to a flare and associated CME to demonstrate that while the filament itself did not appear to erupt, it underwent significant dynamic motion and morphological changes in the early stages of the CME initiation. The cospatial and cotemporal correspondence with flare-associated brightenings at other wavelengths allowed these authors to conclude that models that allow reconnection high above the core region are more relevant to the CME initiation process.

The eruption of an active region filament on 2002 May 27 was accompanied by a flare of *GOES* class M2.0, but with no detectable CME. The early development of the filament was typical of the initiation phase of eruptive filaments. However, in this case the filament flux rope underwent a kinking motion that effectively terminated the rise of the filament at a height of some 80 Mm above the photosphere (J03). The observed writhing motion has led some modelers to consider kink-unstable flux rope configurations in an attempt to explain the dynamics of this intriguing event (e.g., Török et al. 2004a, 2004b).

J03 showed that, even though the filament failed to erupt, significant energy release occurred in association with the complex filament dynamics. This energy release resulted in a number of radiative signatures in the corona, suggesting the possible presence of magnetic reconnection in the magnetic field overlying the filament prior to the filament erupting phase. Most notably, these radiative signatures included hard X-ray emission in the 12–25 keV range detected by *RHESSI*. J03 therefore concluded that two conditions are required for an eruption to occur: reconnection in the low corona (possibly above the filament) and open or opening fields. If correct, this has important consequences for models of CME initiation.

As part of an ongoing study of the association of energetic particle production with filament activation, we revisited the J03 failed eruption event and find significant additional information in the behavior of the coronal hard X-ray emission, which serves to clarify the dynamic evolution of the filament flux rope and to refine the physical interpretation. The discovery of additional coronal emission and its implications for models of filament eruptions provides the motivation for the present study. We discuss our observations and data analysis in § 2, characterize the spatial and temporal evolution of this event in § 3, and present a discussion and our interpretation in § 4.

2. DATA ANALYSIS AND OBSERVATIONS

One of the key aspects of the interpretation of J03 was the discovery of a coronal source of 12–25 keV hard X-ray emission

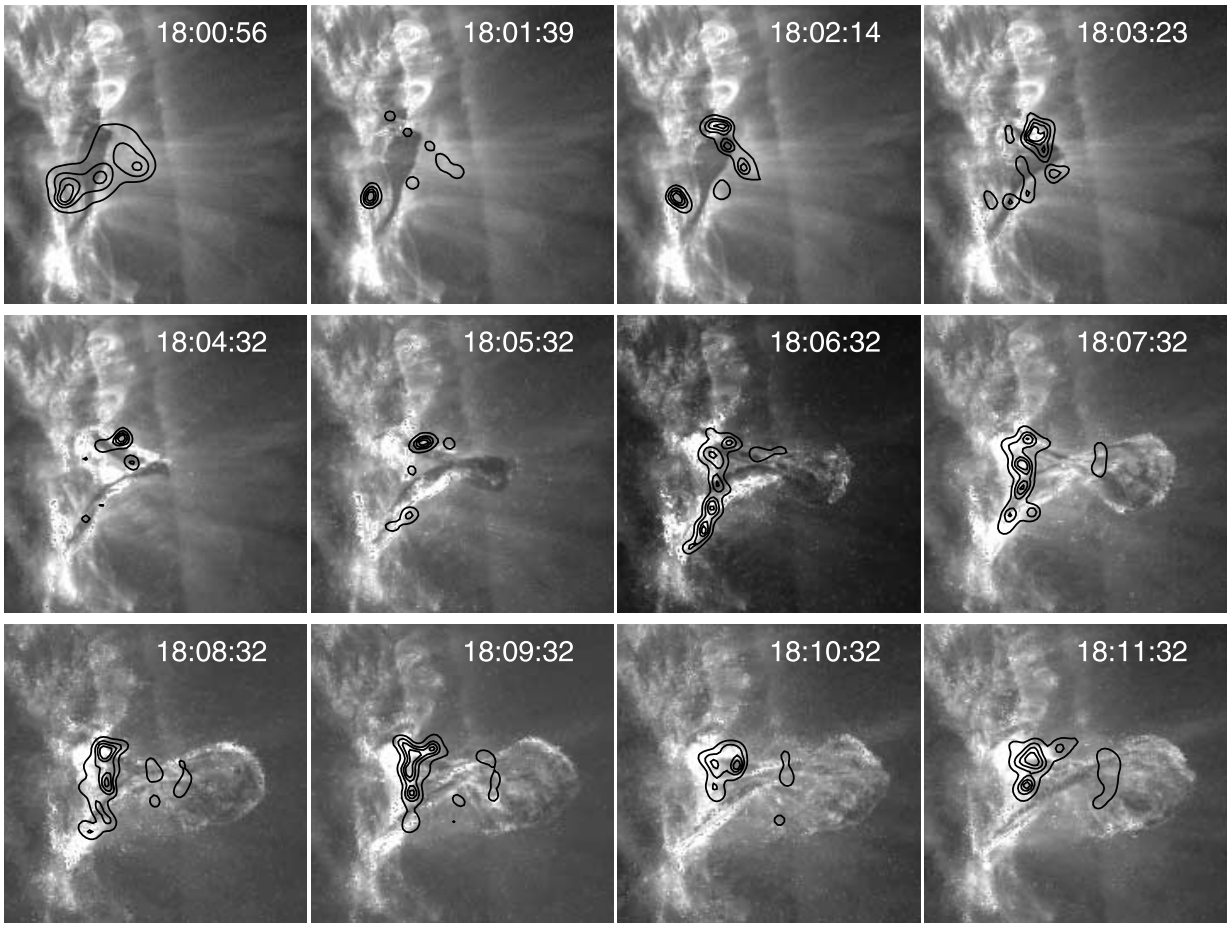

FIG. 1.—Temporal evolution of the active filament eruption seen in *TRACE* 195 Å images on 2002 May 27. The contours show the 12–25 keV hard X-ray emission from *RHESSI*. The apex of the filament lies approximately 80 Mm above the solar surface.

early in the event (18:00:00–18:02:30 UT) at a location some 7–9 Mm above the filament. This site of coronal hard X-rays is interpreted as the location of energy release by J03, a conclusion borne out by subsequent emission in the blue wing of Hα and the EUV at 195 Å at the same location. To quote J03 "the hard X-rays, Hα blue wing, and Fe XII 195 Å emissions all showed compact activity in sequence at the same location." The *RHESSI* hard X-ray image reconstruction performed by J03 utilized the CLEAN algorithm (see Aschwanden et al. 2004) with a 40 s integration time, and was restricted to the early period of activity in this event.

RHESSI is a rotating modulation collimator (Lin et al. 2002) from which hard X-ray images can be produced via a detailed analysis of the received modulation patterns (see Hurford et al. 2002 for details). While a number of image reconstruction techniques are available, we choose to work with the Pixon reconstruction method (Metcalf et al. 1996) due to the significantly better photometry that it provides. This allows for a direct comparison to the J03 results while allowing better time resolution (we use 12–40 s depending on the count rates and attenuator state) and the detection of fainter sources later in the event. We concentrate, in this study, on *RHESSI* data in two energy bands (12–25 keV and 25–50 keV), with a spatial resolution defined by the lowest grid used, which here is grid 3, corresponding to a resolution of $\sim 7''$. The *TRACE* data used in this study is the same sequence of 195 Å images used by J03. Because of an unknown flexing of the *TRACE* metering tube, which affects the true pointing knowledge of the *TRACE* telescope (see Fletcher et al. 2001), we perform a co-alignment of the *TRACE* and *RHESSI* images using the identification of similar structure in EIT 195 Å data. We assume that the pointing of EIT and *RHESSI* are known accurately. The correction to the *TRACE* pointing in this case is approximately $6''$.

In addition to *RHESSI* and *TRACE*, we use He I ($\lambda = 1083$ nm) spectral line data from the Chromospheric Helium Imaging Photometer (CHIP) at the Mauna Loa Solar Observatory (MLSO) to obtain line-of-sight velocity observations of the filament mass.

3. SPATIAL AND TEMPORAL EVOLUTION OF EUV AND HARD X-RAY EMISSION

Figure 1 shows the time development of the filament as observed in the *TRACE* 195 Å channel from 18:00:56 to 18:11:32 UT. Also shown is the 12–25 keV hard X-ray emission overlain as contours. The filament evolves quite dramatically over a period of $\sim$10 minutes, with a slow rise phase from 18:00:56 to 18:02:14 UT being followed by a rapid expansion with a distinct kinking motion evident. The filament itself appears to be confined, reaching a maximum height of $\sim$80 Mm. Beyond $\sim$18:10 UT the filament structure has effectively stopped rising, and most of the dynamic motion is in the form of material draining down the legs of the filament to the chromosphere. There is also some evidence for an untwisting motion as the filament drains (see below). A movie of the filament evolution can be found at the authors' Web site.[1]

[1] See movie at http://trace.lmsal.com/POD/movies/T195_020527_18M2.mov.

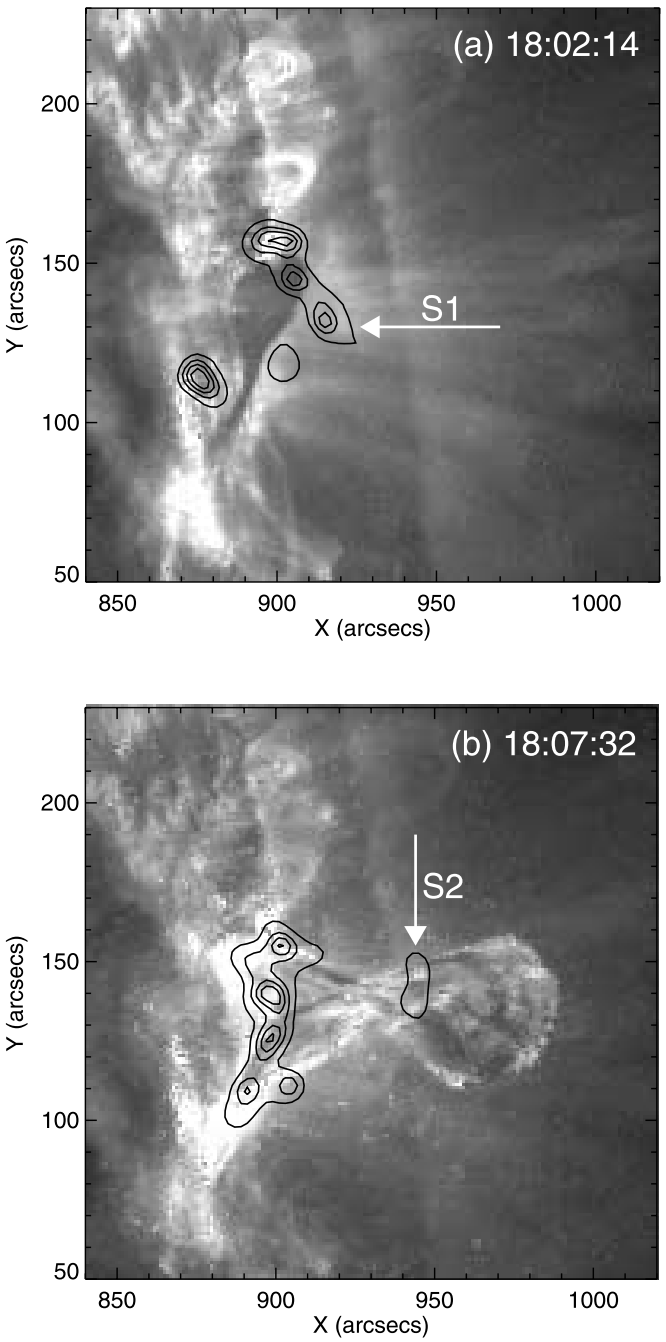

FIG. 2.—Coronal hard X-ray sources, marked by arrows, in relation to the filament. (*a*) Source S1, identified by J03, lies above the filament prior to the filament eruption. (*b*) Source S2, located at the projected crossing point of the two filament legs. The integration time of the *RHESSI* data, centered on the time of the *TRACE* image, is 40 s in (*a*), to match the J03 analysis, and 12 s in (*b*).

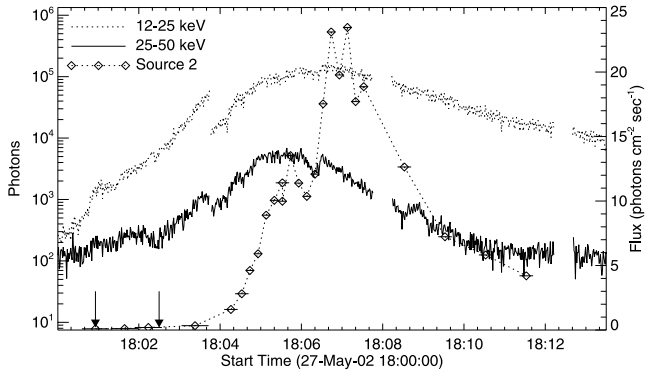

FIG. 3.—Light curves of *RHESSI* hard X-ray emission. The dotted and solid lines show the time evolution of the 12–25 and 25–50 keV emission, respectively, from the whole flare (in photons). The diamonds indicate the time evolution of the 12–25 keV coronal source (S2; photons cm^{-2} s^{-1}). The arrows delimit the time over which the hard X-ray coronal source (S1) was detected. The gaps in the whole flare light curves are due to attenuator switches in *RHESSI*.

The hard X-ray emission is evident from the onset of the filament activation, with the 12–25 keV emission beginning around 18:00:20 UT and the 25–50 keV emission starting some two minutes later at ~18:02:30 UT. In addition to the usual hard X-ray footpoints, a coronal source (S1) in the 12–25 keV band, first identified by J03, is clearly evident above the erupting filament at spatial location 913″ W, 130″ N, relative to disk center (see Fig. 2), beginning at 18:00:56 UT, and lasting approximately 3 minutes. (J03 have the coronal source disappearing after 18:02:30 UT, but Fig. 1, which was generated by the Pixon reconstruction method, sees signs of it lasting until as late as ~18:03:30 UT.)

Following the initial evolution the filament develops a dramatic kink; the footpoint structures evolve, showing multiple interaction sites in the chromosphere (see frame at 18:06:32 UT). Meanwhile, the coronal emission fades from the initial energy release site above the filament, as the filament erupts through its kink phase. A second, independent coronal hard X-ray source (S2) forms at location 948″ W, 134″ N, cospatial with the projected crossing point of the kinked filament structure (Fig. 2). This additional hard X-ray source, not discussed by J03, lies approximately 25 Mm above the earlier J03 source, S1, but below the apex of the now-confined filament. Figure 2 shows the spatial and temporal differences between the two coronal hard X-ray sources detected by *RHESSI*.

The time development of source S2 indicates that it appears approximately 1–2 minutes after the initial source S1 disappears and is closely associated with the writhing motion exhibited by the filament. Figure 3 shows that source S2 develops around 18:03:40 UT (shortly after the disappearance of coronal source 1), peaking at ~18:07:00 UT, in agreement with the peak 12–25 keV emission of the flare as a whole, and ~30 s after the flare peak in the 25–50 keV emission. The coronal source decays quickly over the next 3–4 minutes. Throughout its appearance, source S2 remains at the same physical location and same position relative to the draining filament. The association of coronal source S2 with the projected crossing point of the two filament legs suggests a scenario whereby magnetic reconnection of oppositely directed field, presumably in a current sheet that forms between the inner portions of the adjacent filament legs, powers further energy release, generating the observed hard X-ray emission.

The overall dynamical behavior of the filament is further illuminated by analysis of the MLSO CHIP line-of-sight velocity data, which has a 3 minute cadence, in conjunction with the image sequence from *TRACE*. The early evolution of the filament from 18:05 to 18:08 UT is dominated in the velocity data by the rapid expansion of the confined structure. This expansion is indicated by a growing dark (negative velocity) region, signifying the expansion of the structure toward the observer, together with a narrow positive velocity feature, signifying the observed portion of the flux rope that is expanding away from the observer. As the expansion ceases and the filament maintains its confined configuration, the velocity data indicate a combination of motions

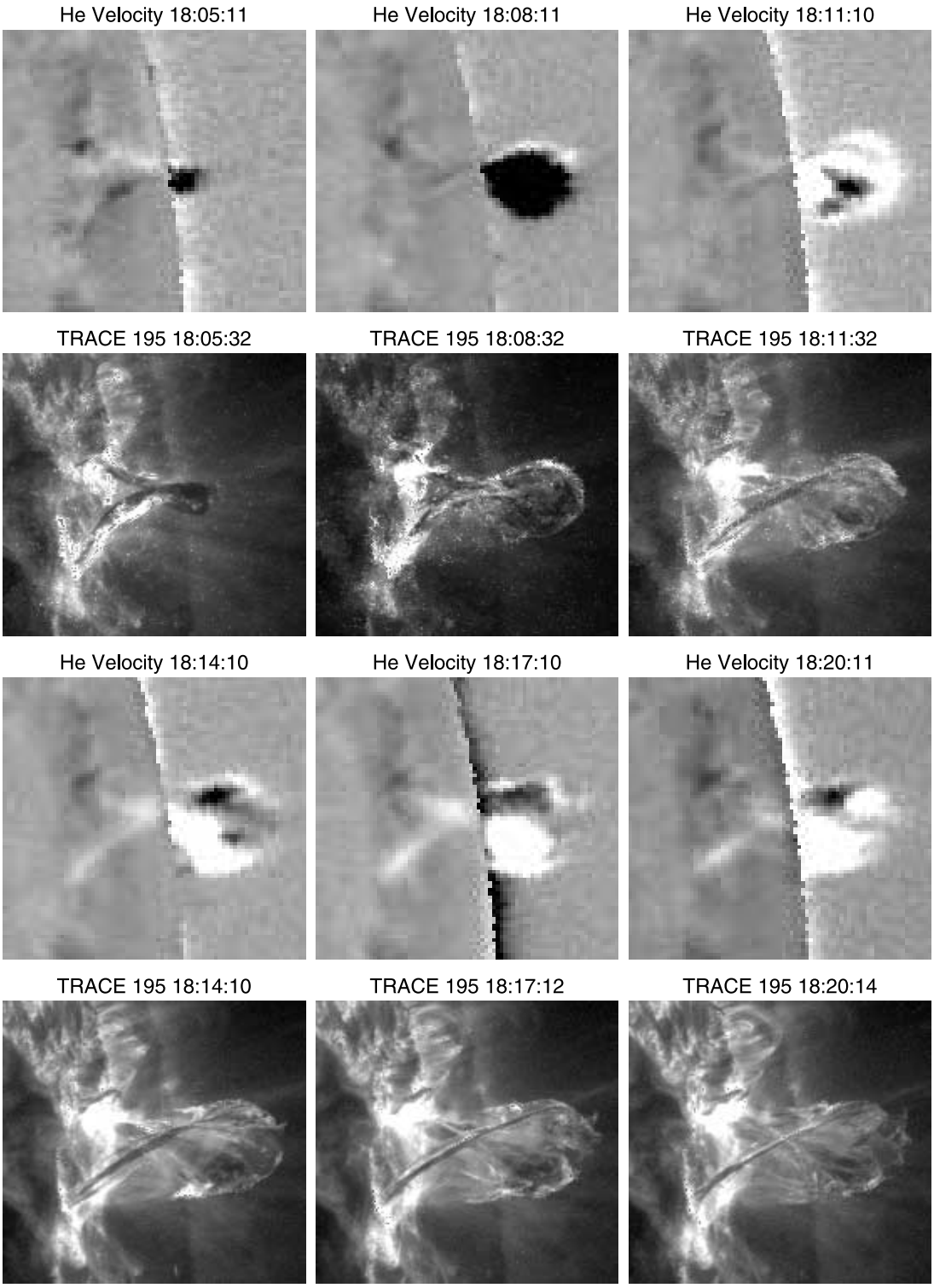

FIG. 4.—Correspondence between MLSO CHIP He 1083 nm line-of-sight velocity data and the *TRACE* 195 Å observations of the kinking filament. In the velocity data (*first and third rows*), black (white) indicates velocity toward (away from) the observer. In the *TRACE* data (*second and fourth rows*) black (white) indicates absorbing (emitting) plasma. [*See the electronic edition of the Journal for a color version of this figure and mpeg animations of expansion and untwist*.]

resulting from an apparent "untwisting" of the entire apex of the filament (18:14–18:20 UT) and the draining of filament material evident in the *TRACE* 195 Å data. The untwisting is evident in the *TRACE* movies, as well as in the velocity data. The CHIP observations in row 3 of Figure 4 show a characteristic dipolar pattern, with the front and southerly part of the filament apex moving away from us and the back and northerly part moving toward us (opposite to that detected during the expansion phase).

4. DISCUSSION AND INTERPRETATION

The results presented in the previous section provide insight into the nature of filament activation and eruption. The "failed" eruption discussed here places constraints on models of CME

initiation and yields important clues to the interaction between filaments and their surrounding magnetic field.

The key distinction between the present analysis and that performed previously by J03 is the use of the Pixon reconstruction algorithm for the *RHESSI* hard X-ray data, which provides better photometry than the CLEAN procedure used by J03, allowing shorter integration times and longer coverage of the event into its hard X-ray decay. In addition to confirming the J03 detection of a coronal source above the filament at the onset of the activation, we highlight a second coronal source evident at a later time lying below the erupted filament structure, not discussed by J03, but evident at a low level in their Figure 1*g*. The presence of the hard X-ray emission in the corona suggests the local interaction of fast particles with the ambient medium, where the particles are assumed to be produced locally in an energy-release site, possibly driven by magnetic reconnection. The earlier coronal hard X-ray source (S1) lying above the filament, prior to the rapid expansion phase of the filament, possibly indicates the opening of magnetic field, or the significant reduction of the magnetic tension in the overlying field, allowing the filament to rise (see also J03). The enhanced detection of a second hard X-ray source in the corona (S2) situated at the projected crossing point of the kinking filament legs (see Figs. 1 and 2) indicates the possible interaction of the adjacent filament legs brought together by the kinking action of the eruption. The reconnection of the magnetic field in this internal region results in a local energy release producing the hard X-ray emission and the localized heating of plasma indicated by the EUV and Hα brightenings discussed by J03.

The full scenario painted by these observations, then, is that reconnection above the energized filament opened, or significantly weakened, the overlying field, allowing the filament to begin to erupt. The strong line-tying of the filament footpoints, the kinking motion of eruption, and the form of the overlying magnetic field serve to confine the filament, restricting any subsequent ejection into the corona. The kinking motion also serves to bring oppositely directed magnetic field from the two filament legs together, creating the conditions for magnetic reconnection and further energy release powering the hard X-ray emission (both in the corona and at the chromospheric hard X-ray footpoints) and localized plasma heating.

The initial evolution, in which the energy release signalled by the hard X-ray emission in the corona (source S1) would seem to indicate magnetic reconnection in the field overlying the filament, does not fit with any of the dipped field model scenarios discussed by Gilbert et al. (2001). Reconnection above the arcade in the dip models results in the formation of an inverse-polarity flux rope above the filament, but the dip supporting the filament maintains its integrity and does not erupt. The inverse-polarity flux rope models of Gilbert et al. (2001) fare no better in explaining the observed behavior, as they do not support a situation in which the filament eruption is initiated by reconnection above the flux rope containing the filament. However, the scenarios outlined by Gilbert et al. (2001) do not allow for the kinking motion of the "failed" filament eruption discussed here, nor do they attempt to explain how a filament might be confined. One possibility might be that the filament forms in a normal-polarity flux rope, which becomes unstable as a result of reconnection in the overlying arcade. The subsequent evolution depends on the strength of the overlying field and the driving mechanism. In principle, a rising filament could lead to the formation of a current sheet underneath, which then reconnects to cause the filament to erupt. This scenario combines facets of the popular breakout (Antiochos et al. 1999) and catastrophe (Lin & Forbes 2000) models.

Most models addressing the activation of solar filaments and its role in the production of flares and CMEs focus on the eruption process and the subsequent response of the coronal field and plasma. A variety of theoretical models have been proposed to explain the impulsive onset and initial evolution of solar eruptions (see Lin et al. 2003). However, the application to partial or confined eruptions is a relatively recent topic of interest (e.g., Gibson & Fan 2006). Recently Török & Kliem (2005; hereafter TK05) used a flux rope instability model to simulate the dynamic behavior of the 2002 May 27 "failed" eruption event studied here. Motivated by the observations of J03, TK05 modeled the confined eruption of a helical flux rope driven by the ideal kink instability (see also Titov & Démoulin 1999; Török et al. 2004a, 2004b). In this model the average twist of the flux rope is assumed to be quite large, $\Phi = 5\pi$, in order to reproduce the observed helical shape of the rising filament evident in Figure 1.

The TK05 model reproduces both the observed development of the kinking structure and the rise profile of the filament reasonably well. More interestingly, their model allows for the same configuration to generate a fully erupting filament by simply modifying the form of the overlying magnetic field. The authors argue that this points to the kink instability as a prime driver of solar eruptions, and the response of the filament to this instability is determined by how quickly the overlying magnetic field declines with height.

In addition to the successful reproduction of the dynamical evolution of the 2002 May 27 event, the TK05 simulations also provide the conditions necessary to foster energy release in the solar corona. While they do not directly address the energy release implied in the production of hard X-rays nor its role in the ensuing dynamics, they do discuss the formation of the current sheets generated by the kink instability driving the flux rope eruption. In particular, the instability results in the formation of a helical current sheet wrapped around the kinking and rising flux rope and a vertical current sheet below the flux rope (Török & Kliem 2004a). The vertical current sheet formed by the writhing motions has no counterpart in the cylindrical flux tube approximations, and its presence below the rising unstable magnetic flux provides a natural explanation for the energy release implied by the coronal hard X-ray source S2. The early coronal hard X-ray source (S1), identified by J03, indicates the presence of magnetic reconnection in the field overlying the filament, presumably in the helical current sheet discussed by TK05. The TK05 simulations are performed in ideal MHD and do not directly address the effects the energy release might have on the subsequent dynamics nor how they might alter conclusions regarding the role played by the form of the overlying field.

The velocity data obtained from the MLSO/CHIP instrument indicated a period of rapid expansion as the flux rope writhed early in the event and an apparent untwisting at the end of the event once it had ceased to rise. This untwisting is also evident in the *TRACE* movies of this event. These observations also support the kink-unstable flux rope model of Török & Kliem. The initial expansion reflects the translational motion of the flux rope during its strong writhing phase, while the apparent untwisting is consistent with the relaxation phase discussed, briefly, in Török & Kliem (2004b) where the flux rope relaxes to its initial circular shape.

The dynamics of the 2002 May 27 failed eruption event and the concomitant coronal hard X-ray emission provide important

insight into the filament eruption process. The new observations presented here add to the complexity of the event but compare favorably with extant models where the filament dynamics are driven by the kink instability.

The authors are grateful to the *TRACE*, *RHESSI*, and MLSO instrument teams for the excellent data provided to the solar physics community. This work was partially supported by an NSF SHINE grant, ATM 03-53345.

REFERENCES

Antiochos, S. K., DeVore, C. R., & Klimchuk, J. A. 1999, ApJ, 510, 485
Aschwanden, M. J., et al. 2004, Sol. Phys., 219, 149
Fletcher, L., Metcalf, T. R., Alexander, D., Brown, D. S., & Ryder, L. A. 2001, ApJ, 554, 451
Gibson, S. E., & Fan, Y. 2006, ApJ, 637, L65
Gilbert, H. R., Holzer, T. E., Burkepile, J. T., & Hundhausen, A. J. 2000, ApJ, 537, 503
Gilbert, H. R., Holzer, T. E., Low, B. C., & Burkepile, J. T. 2001, ApJ, 549, 1221
Hurford, G. J., et al. 2002, Sol. Phys., 210, 61
Ji, H., Wang, H., Schmahl, E. J., Moon, Y.-J., & Jiang, Y. 2003, ApJ, 595, L135 (J03)
Lin, J., & Forbes, T. G. 2000, J. Geophys. Res., 105, 2375
Lin, J., Soon, W., & Baliunas, S. L. 2003, NewA Rev., 47, 53
Lin, R. P., et al. 2002, Sol. Phys., 210, 3
Martin, S. F. 1998, Sol. Phys., 182, 107
Metcalf, T. R., et al. 1996, ApJ, 466, 585
Pevtsov, A. A. 2002, Sol. Phys., 207, 111
Sterling, A. C., Moore, R. L., Qiu, J., & Wang, H. 2001, ApJ, 561, 1116
Titov, V. S., & Démoulin, P. 1999, A&A, 351, 707
Török, T., & Kliem, B. 2004a, in Proc. SOHO 15 Workshop—Coronal Heating, ed. R. W. Walsh et al. (ESA SP-575; Paris: ESA), 56
———. 2004b, A&A, 413, L27
———. 2005, ApJ, 630, L97 (TK05)